Neutron Star Astrophysics at the Crossroads: Magnetars and the Multimessenger Revolution
Proceedings IAU Symposium No. 363, 2023
E. Troja & M. G. Baring, eds.
doi:10.1017/S1743921322002332

The search for Continuous Gravitational Waves: the journey to discovery

Paola Leaci

Dip. di Fisica, Università di Roma "Sapienza" and INFN Sezione di Roma
P.le A. Moro 2, I-00185 Rome, Italy
email: paola.leaci@roma1.infn.it

Abstract. Continuous gravitational Waves (CWs) are a very promising, not yet detected, and interesting class of persistent and semi-periodic signals. They are emitted mainly by rapidly rotating asymmetric neutron stars, with frequencies that are well covered by the [10-3 000] Hz range of the advanced LIGO-Virgo detectors. Due to the expected small degree of asymmetry of a neutron star, the search for this kind of signals is extremely challenging, and can be very computationally expensive when the source parameters are not known or not well constrained. CW detection from a spinning neutron star will allow us to characterize its structure and properties, making this source an unparalleled laboratory for studying several key issues in fundamental physics and relativistic astrophysics, in conditions that cannot be reproduced on Earth. The most recent methodologies used in CW searches will be discussed, and the latest results from the third advanced LIGO-Virgo observational run will be presented. A summary of future prospects to feasibly detect such feeble signals as the detector performance improves, and ever-more-sensitive and robust data-analysis algorithms are implemented, will be also outlined.

Keywords. gravitational waves, interferometers, data analysis, neutron stars, black hole physics, detectors.

1. Introduction

After the first transient gravitational-wave observation on September 14, 2015 [Abbott *et al.* (2016)], several other compact-binary-coalescence events have been detected [Abbott *et al.* (2019); Abbott *et al.* (2021)]. Here we focus on a different class of unobserved gravitational-wave signals, which is represented by long-lasting continuous waves (CWs) that are expected to be emitted by rapidly rotating neutron stars with non-axisymmetric deformations [Owen (2005)]. We expect $\mathcal{O}(10^8)$ of these sources to exist in the Galaxy [Camenzind (2007)], but only $\sim 3\,000$ neutron stars (mostly pulsars) have been electromagnetically observed [ATNF Catalogue]. Roughly 1 300 of these observed radio pulsars are located in binary systems, and have rotation rates such to possibly emit CWs in the advanced LIGO-Virgo sensitivity band.

The observation of CWs from a spinning neutron star will unveil its structure and properties, making this source an exceptional laboratory for studying crucial issues in fundamental physics and relativistic astrophysics, in conditions that cannot be reproduced on Earth. The search for such class of signals is, however, quite difficult due to their expected weakness, and can be very computationally expensive when the source parameters are not known or not well constrained.

After a brief recap on CWs and how a search for these feeble signals can be performed, we present the most up to date results from different kinds of CW analyses [Riles (2017)] using data from the the latest LIGO-Virgo third observing run (O3) [Abbott *et al.* (2020)],

which spanned the time period April 1, 2019 – March 27, 2020, with a commissioning break in October 1–31, 2019.

2. The Physics of CW signals

CWs require long integration times, typically of the order of months or years, to accumulate a Signal-to-Noise Ratio (SNR) sufficient for detection [Jaranowski (1998)]. Due to a variety of mechanisms [Lasky (2015)], neutron stars are expected to emit long-lived CWs, and depending on the amount of information that one knows about the source, there are different types of searches one can perform: *(i)* targeted searches, where the source phase parameters (i.e. sky location, rotational frequency and frequency derivatives, i.e. (spindown)) are assumed to be known with great accuracy (e.g. the Crab and Vela pulsars); *(ii)* directed searches, where sky location is known while frequency and frequency derivatives are unknown (e.g. Cassiopeia A, SN1987A, Scorpius X-1, galactic center, globular clusters); *(iii)* all-sky searches for unknown neutron stars, where none of the above parameters is known.

The CW signal is received at the detector with a frequency modulation due to the Doppler effect caused by the Earth motion and, for sources in a binary system, also by the binary orbital motion, e.g., [Leaci (2017); Singhal (2019); Abbott *et al.* (2021a)]. Furthermore, these signals have an amplitude and phase modulation caused by the time varying detector response function towards a precise sky direction.

The measured strain amplitude h_0 on Earth is given by

$$h_0 = \frac{4\pi^2 G}{c^4}\frac{I_{zz} f^2 \varepsilon}{d}, \tag{2.1}$$

where f is the frequency of the emitted gravitational-wave signal (which is also twice the rotational frequency of the star), G is Newton's constant, c is the speed of light and d is the distance to the star. The distribution of the ellipticity ε for neutron stars is uncertain and model dependent since the breaking strain for a neutron star crust is highly unknown (see, e.g., [Ushomirsky *et al.* (2000); Horowitz *et al.* (2009)] for further discussion).

In general, the strategy used to extract these faint signals -from the interferometer noisy data- is based on a coherent (i.e. the phase information is used) matched-filtering analysis, consisting in correlating the data against a template, which models the signal amplitude and phase evolution over time and maximizes the SNR [Jaranowski (1998); Leaci (2015)]. However, the computational requirements of the search increase dramatically with the time baseline, and wide-frequency-band all-sky searches become computationally challenging [Brady (1998)]. Hence, hierarchical procedures, which alternate coherent and incoherent steps, have been proposed [Astone *et al.* (2014); Abbott *et al.* (2018); Krishnan *et al.* (2014)].

In the following we discuss the application of some of these algorithms to real LIGO-Virgo O3 advanced detector data.

3. O3 CW search highlights

CWs from known/unknown isolated/binary neutron stars have yet to be detected. However, strict upper limits on the gravitational-wave strain amplitude have been reached.

We present some of the most recently released and sensitive results obtained from the O3 LIGO-Virgo observing run.

All-sky search for CWs from isolated neutron stars in early O3 data

This search analyzes the first six months of the O3 (O3a) data set using the PowerFlux program (see [Abbott *et al.* (2018)] and references therein), where the strain power is

https://doi.org/10.1017/S1743921322002332 Published online by Cambridge University Press

summed over many Short Fourier Transforms after correcting for Doppler modulations. This is done for a large bank of templates based on sky location, frequency, frequency derivative and source orientation. The search paramter space consists into a $[20,\ 2\,000]$ Hz and $[-1,\ 0.1] \times 10^{-8}$ Hz/s frequency and frequency derivative regions, respectively. CW candidates having high values of SNR are followed up in a multi-stage search with increasing levels of adequate coherence at each stage to further increase the expected SNR. Candidates surviving at all stages are deeply examined to confirm/exclude their credibility as CW sources, with further follow-up carried out in the full O3 data set.

No candidates have survived deep scrutiny in this search. Hence, we set stringent 95% confidence-level upper limits on the strain amplitude as a function of the frequency, which we report in Fig. 1 (a) [Abbott *et al.* (2021b)], with the lowest value being 1.4×10^{-25}. As we note, these upper limits improve with respect to previously published all-sky results, reaching a factor 2 at higher frequencies, and being the most constraining upper limits we have until today over most of the search parameter space.

In Fig. 1 (b) we show the astrophysical reach of the search for different neutron-star deformations, i.e. ellipticity values [Abbott *et al.* (2021b)]. In particular, at 2 000 Hz, we are sensitive to neutron stars with an equatorial ellipticity of $\varepsilon \sim 4 \times 10^{-7}$ and as far away as 6 kpc for favorable spin orientations. For a higher ellipticity $\varepsilon \sim 10^{-6}$, and favorable spin orientations, we are sensitive to neutron stars beyond the galactic center. Finally, our results are sensitive to $\varepsilon \sim 10^{-5}$, which is the maximum ellipticity that a conventional neutron star can theoretically support, at frequencies above 100 Hz star rotation frequency (i.e., 200 Hz gravitational-wave frequency) within 3 kpc.

Constraints on CWs from the energetic young X-ray pulsar PSR J0537-6910

Another important search consisted into targeting the X-ray pulsar PSR J0537-6910, which has the largest spindown luminosity of any pulsar and is quite active with regards to glitches. A time-domain Bayesian approach in a combination of O2 and O3 data has been used [Abbott *et al.* (2021c)], together with NICER observations that provided detailed information on spin frequency and evolution. Analyzing its long-term and inter-glitch braking indices, one can obtain fascinating evidence that its spindown energy budget may include gravitational-wave emission from a time-varying mass quadrupole moment. Its 62 Hz rotation frequency also puts its potential gravitational-wave emission in the most sensitive band of the advanced LIGO-Virgo detectors. Since no detection can be claimed, we proceed to set upper limits: our constraints reach below the gravitational-wave spindown limit (for the first time for this pulsar) by more than a factor of 2 and limit gravitational waves to account for less than 14% of the spindown energy budget. The fiducial equatorial ellipticity is limited to less than about 3×10^{-5}, which is the third best constraint for any young pulsar [Abbott *et al.* (2021c)]. This is summarized into the posterior probability distribution plot that is shown in Fig. 2.

Constraints on CW emission due to r-modes in the glitching pulsar PSR J0537-6910

The source PSR J0537-6910 has been targeted to search also for r-modes (i.e., toroidal fluid oscillations within a neutron star) from the full O3 data set and using the NICER ephemeris, where three glitches of J0537 have been detected during the O3 run.

Two search methodologies have been employed: the time domain $\mathcal{F}/\mathcal{G}$-statistic method and the 5-vector method [Abbott *et al.* (2021d)]. The first one consists into performing a coherent search of time domain segments via the $\mathcal{F}$-statistic [Jaranowski (1998)] and $\mathcal{G}$-statistic [Jaranowski (1998)] approaches, while the second one into running a 5-vector narrow-band search [Mastrogiovanni *et al.* (2017)], where a possible mismatch between the actual gravitational-wave frequency and the value inferred from electromagnetic (EM) observations can occur. This can be due to either errors in the EM measurements or in the presence of differential rotation, if the gravitational-wave signal is emitted by the inner

https://doi.org/10.1017/S1743921322002332 Published online by Cambridge University Press

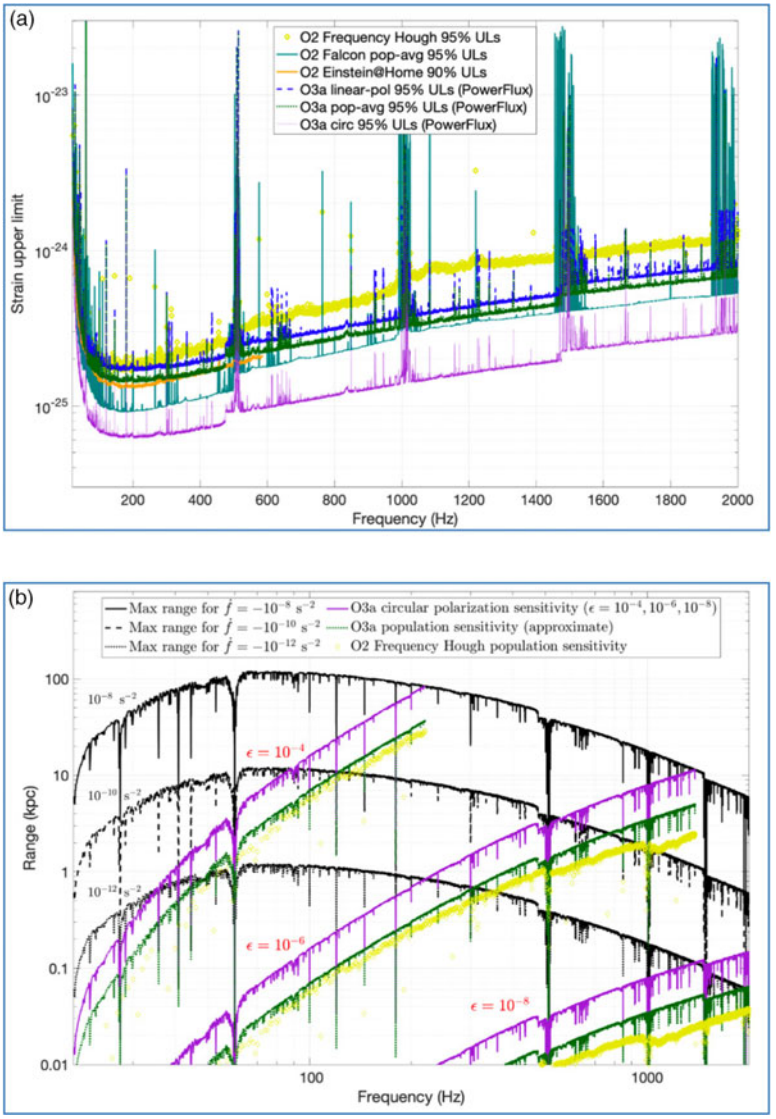

Figure 1. Panel (a): Upper limits on the gravitational-wave strain amplitude for the O3a data set and for previous O2 run analyses (see Abbott *et al.* (2021b) for more details). The blue (magenta) curve shows linearly (circularly) polarized 95% confidence-level upper limits in analyzed (62.5 mHz, 125 mHz, 250 mHz) sub-bands for the broad (20-475 Hz, 475-1475 Hz, 1475-2000 Hz) search bands. The green curve shows approximate population-averaged all-sky upper limits inferred from the circularly polarized limits. **Panel (b)**: Astrophysical ranges (in kpc) of the PowerFlux search for neutron stars spinning down solely due to gravitational radiation under different assumptions. The three sets of purple, green and yellow curves correspond to the ranges for which the O3a circular-polarization, O3a population-averaged and O2 population-averaged Frequency Hough [Abbott *et al.* (2019)] upper limits apply for ellipticities values of $\varepsilon = 10^{-4}$, 10^{-6}, 10^{-8} [Abbott *et al.* (2021b)].

parts of the star rather than by the crust, or in case of free precession. The standard 5-vector narrow-band search has been adapted to perform a semi-coherent search, where intra-glitch periods have been studied coherently and the results are later on combined incoherently. The search frequency region ranges from 86 Hz to 97 Hz.

https://doi.org/10.1017/S1743921322002332 Published online by Cambridge University Press

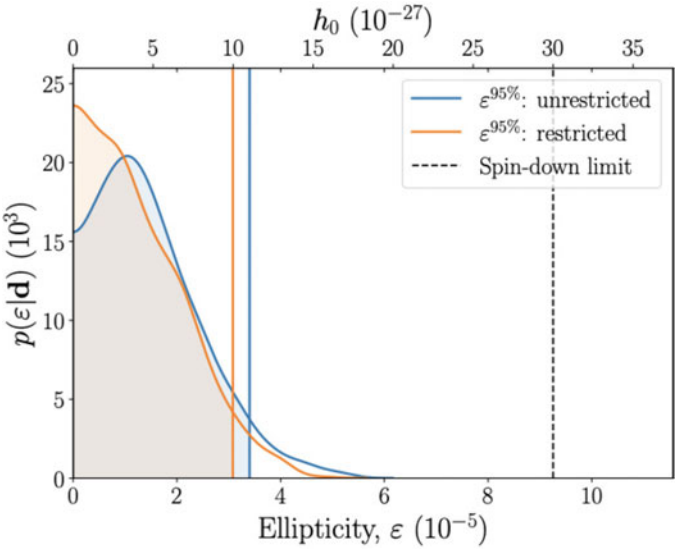

Figure 2. Posterior probability distribution for ellipticity and h_0 for the analyses with unrestricted (i.e., an isotropic prior on the axis direction) and restricted (i.e., Gaussian) priors on the pulsar orientation. The 95% upper limits are represented by the straight colored lines, while the spindown limit is given by the straight black line [Abbott *et al.* (2021c)].

No significant CW candidates have been found. Hence, we have calculated upper limits on the r-mode amplitude α [Abbott *et al.* (2021d)] for two different equations of state:

$$\alpha = \sqrt{\frac{5}{8\pi}} \frac{c^5}{G} \frac{h_0}{(2\pi f^3)} \frac{d}{MR^3 J} \approx 0.017 \left(\frac{90 \text{ Hz}}{f}\right)^3 \frac{h_0}{10^{-26}}, \tag{3.1}$$

where M and R are the mass and radius of the star, respectively, while J is the dimensionless canonical angular momentum of the r-mode [Abbott *et al.* (2021d)].

Figure 3 (a) shows results for the stiffest, causally limited equation of state with crust, while results for the softest case, the WFF1 EoS, are plotted in Fig. 3 (b). The dotted lines represent the amplitude α that would correspond to the spindown limit [Abbott *et al.* (2021d)].

These results favour soft equations of state and are consistent with stars having a mass smaller than 2 solar masses, and being spun down by gravitational-wave emission due to r-modes.

Search for CWs from accreting millisecond X-ray pulsars

A relevant directed analysis has been performed searching for CWs from 20 accreting millisecond X-ray pulsars (listed in Fig. 4) with well-constrained rotational frequencies and orbital elements coming from EM observations of outburst events. The search frequency sub-bands are centered on $\{1, 4/3, 2\}$ f^* for every target. The search pipeline we use allows for spin-wandering via a hidden Markov model [Middleton, *et al.* (2020)], which relies on the Viterbi algorithm to effectively track the most likely spin history, and the $\mathcal{J}$-statistic [Suvorova, *et al.* (2017)], which tracks the orbital phase of the binary calculating the likelihood a CW is present in the detector data.

No significant candidates could be identified. Hence, we estimate 95% confidence level upper limits on the gravitational-wave strain amplitude, which we show in Fig. 5. From those we can deduce that the stringent constraints on neutron star ellipticity and r-mode amplitude are $\varepsilon^{95\%} = 3.1 \times 10^{-7}$ and $\alpha^{95\%} = 1.8 \times 10^{-5}$, respectively for the IGR J00291+5934 source [Abbott *et al.* (2021e)].

https://doi.org/10.1017/S1743921322002332 Published online by Cambridge University Press

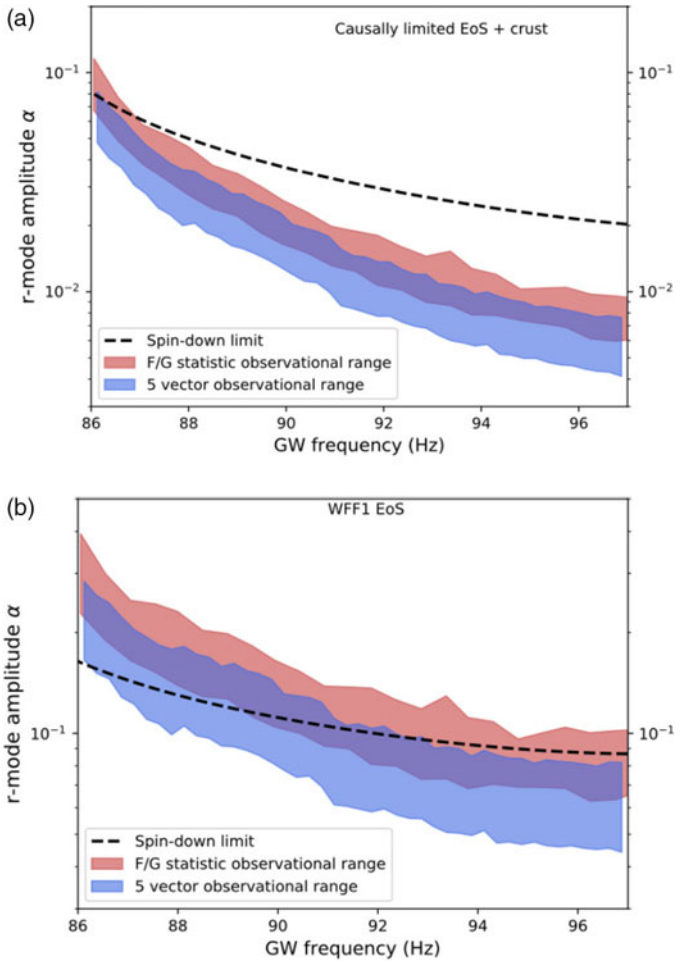

Figure 3. r-mode amplitude upper limits for two equations of state: the stiffest and causally limited equation of state with crust is shown in **Panel (a)**, while the softest case we consider, i.e. the WFF1 equation of state, is shown in **Panel (b)** [Abbott *et al.* (2021d)].

Constraints on dark photon dark matter using O3

Finally, a peculiar search for dark photon dark matter has been also performed over the full O3 data set [Abbott *et al.* (2021f)]. This is motivated by the fact that ultralight dark photon dark matter could cause time-dependent oscillations in the mirrors of the LIGO-Virgo detectors, which would translate into a differential strain. We assume dark photons to be analogous to ordinary photons, i.e. with a vector potential and an associated dark electric field that causes a quasi-sinusoidal force on the detector mirrors.

The search methodologies we used are a cross-correlation [Pierce (2018)] of the two LIGO detector channels and the excess power band-sampled method [Piccinni (2018)] in the strain channels of the LIGO and Virgo detectors.

No evidence of dark photon dark matter with mass $m_A \sim [10^{-14} - 10^{-11}]$ eV/c^2 (corresponding to frequencies from 10 Hz up to 2 kHz) is found. Hence, we provide upper limits on the square of the minimum coupling of dark photons to baryons, i.e. $U(1)_B$ dark matter [Abbott *et al.* (2021f)]. Upper limits we found surpass those of actual dark matter experiments (such as the MICROSCOPE [Berge *et al.* (2018)] and

https://doi.org/10.1017/S1743921322002332 Published online by Cambridge University Press

Target	$f_\star$/Hz
IGR J00291+5934	598.89213099(6)
MAXI J0911−655	339.9750123(3)
XTE J0929−314	185.105254297(9)
IGR J16597−3704	105.1758271(3)
IGR J17062−6143	163.656110049(9)
IGR J17379−3747	468.083266605(7)
SAX J1748.9−2021	442.3610957(2)
NGC 6440 X−2	205.89221(2)
IGR J17494−3030	376.05017022(4)
Swift J1749.4−2807	517.92001385(6)
IGR J17498−2921	400.99018734(9)[b]
IGR J17511−3057	244.83395145(9)
XTE J1751−305	435.31799357(3)[a]
Swift J1756.9−2508	182.06580377(11)
IGR J17591−2342	527.425700578(9)
XTE J1807−294	190.62350702(4)
SAX J1808.4−3658	400.97521037(1)
XTE J1814−338	314.35610879(1)[a]
IGR J18245−2452	254.3330310(1)
HETE J1900.1−2455	377.296171971(5)

Figure 4. Search target list together with the frequency of observed pulsations f^* [Abbott *et al.* (2021e)].

	$h_0^{95\%}$ in each sub-band ($\times 10^{-26}$)		
Target	$f_\star$	$4f_\star/3$	$2f_\star$
IGR J00291+5934	–	7.6	11
MAXI J0911−655	7.7	6.4	7.3
XTE J0929−314	5.1	5.3	6.4
IGR J16597−3704	7.5	–	5.6
IGR J17062−6143	8.1	4.7	4.7
IGR J17379−3747	8.5	7.4	10
SAX J1748.9−2021	9.2	7.7	10
NGC 6440 X−2	6.2	7.2	5.8
IGR J17494−3030	8.3	–	9.0
Swift J1749.4−2807	11	17	24
IGR J17498−2921	7.0	6.6	8.4
IGR J17511−3057	7.5	5.5	6.6
XTE J1751−305	10	8.3	9.7
Swift J1756.9−2508	8.1	8.8	6.3
IGR J17591−2342	9.5	11	14
XTE J1807−294	6.1	5.0	5.6
SAX J1808.4−3658	6.4	6.9	8.8
XTE J1814−338	9.4	6.0	6.9
IGR J18245−2452	9.0	6.3	–
HETE J1900.1−2455	5.6	–	8.4

Figure 5. 95% confidence level upper limits on the gravitational-wave strain amplitude, computed for all sub-bands for every target, except in sub-bands marked with a "dash" due to their high contamination with known instrumental lines [Abbott *et al.* (2021e)].

https://doi.org/10.1017/S1743921322002332 Published online by Cambridge University Press

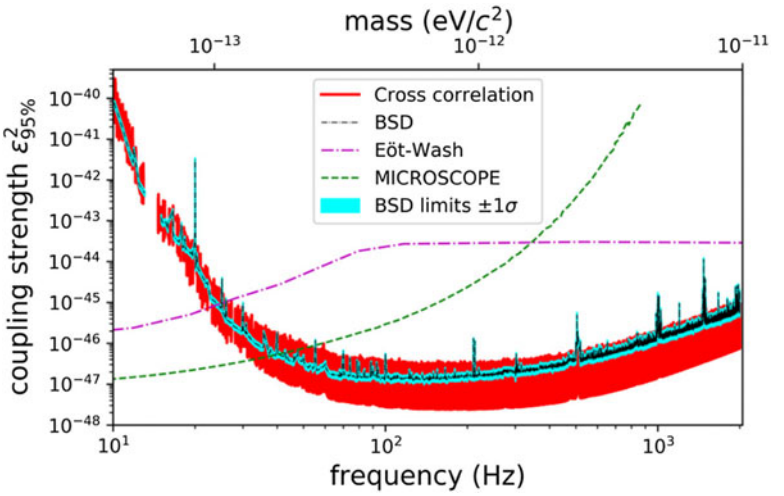

Figure 6. Upper limits on dark photon-baryon coupling, $U(1)_B$ versus frequency for the cross-correlation and band-sampled data searches. These are also compared to those from the MICROSCOPE [Berge *et al.* (2018)] and the Eoet-Wash torsion balance experiment [Schlamminger *et al.* (2008)].

the Eoet-Wash torsion balance experiments) by a factor of ~ 100 in the mass range $m_A \sim [2-4] \times 10^{-13}$ eV/c^2 [Abbott *et al.* (2021f)]. They are depicted in Fig. 6.

4. Conclusions

We have presented some of the best and most recent searches for the yet undetected CWs from the latest O3 advanced LIGO-Virgo detector run. Some of them are motivated by theoretical models and observational evidence. However, all-sky searches for CWs from unknown neutron stars have also been presented.

Additionally, we have introduced a new way to use gravitational-wave interferometers to directly probe the existence of ultralight dark matter.

In none of the cases we could single out a relevant CW candidate, but we provided stringent upper limits on the gravitational-wave strain amplitude. These upper limits help us to start understanding the neutron star physics and shed light on the CW emission mechanisms, although a real picture can be provided only with a CW detection. To facilitate the reach of this goal, we are: *(i)* optimizing search algorithms (porting them to GPUs/Machine Learning whenever necessary) to perform conventional searches as well as challenging searches for long-transient emission from newborn magnetars; *(ii)* improve follow-up methodologies (to be more computationally efficient); *(iii)* getting ready for the most sensitive O4+ run and 3^{rd} generation detectors, such as Cosmic Explorer [Reitze *et al.* (2019)] and Einstein Telescope [Punturo *et al.* (2010)]. As soon as they will be available and come online, we will be able to dig more deeply into the noise and potentially unveil new fascinating, and maybe unexpected, scenarios.

References

Abbott, B. P. *et al.* (The LIGO Scientific Collaboration and the Virgo Collaboration) 2016, *Phys. Rev. Lett*, 116, 061102

Abbott, B. P. *et al.* (The LIGO Scientific Collaboration and the Virgo Collaboration) 2019, *Phys. Rev. X*, 9, 031040

Abbott, B. P. *et al.* (The LIGO Scientific Collaboration and the Virgo Collaboration) 2021, *Phys. Rev. X*, 11, 021053

https://doi.org/10.1017/S1743921322002332 Published online by Cambridge University Press

Owen, Benjamin J. 2005, *Phys. Rev. Lett.*, 95, 211101
Max Camenzind 2007, in: Springer (eds.), *Compact Objects in Astrophysics: White Dwarfs, Neutron Stars and Black Holes* (Science & Business Media: Springer)
ATNF Catalogue, *http://www.atnf.csiro.au/people/pulsar/psrcat/*
Keith, Riles 2017, *Mod. Phys. Lett.*, A32, 1730035
Abbott, B. P. *et al.* (KAGRA Collaboration, LIGO Scientific Collaboration and Virgo Collaboration) 2020, *Living Reviews in Relativity*, 23, 3
Jaranowski P., Krolak A. and Schutz B. 1998, *Phys. Rev. D*, 58, 063001
Lasky P. D. 2015, *Astronomical Society of Australia (PASA)*, 32, e034
Leaci P. *et al.* 2017, *Phys. Rev. D*, 95, 122001
Singhal A. *et al.* 2019, *Class. Quantum Grav.*, 36, 205015
Abbott, R. *et al.* (The LIGO Scientific Collaboration and the Virgo Collaboration) 2021a, *Phys. Rev. D*, 103, 064017
Ushomirsky G., Cutler C. and Bildsten L. 2000, *Mon. Not. Roy. Astron. Soc.*, 319, 902
Horowitz, C.J. and Kadau K. 2009, *Phys. Rev. Lett.*, 102, 191102
Leaci P. and Prix R. 2015, *Phys. Rev. D*, 91, 102003
Brady P. R., Creighton T., Cutler C. and Schutz B. 1998, *Phys. Rev. D*, 57, 2101
Astone P. *et al.* 2014, *Phys. Rev. D*, 90, 042002
Abbott, B. P. *et al.* (The LIGO Scientific Collaboration and the Virgo Collaboration) 2018, *Phys. Rev. D*, 97, 102003
Krishnan B. *et al.* 2004, *Phys. Rev. D*, 70, 082001
Abbott, R. *et al.* (The LIGO Scientific Collaboration and the Virgo Collaboration) 2021b, *Phys. Rev. D*, 104, 082004
Abbott, R. *et al.* (The LIGO Scientific Collaboration and the Virgo Collaboration) 2019, *Phys. Rev. D*, 100, 024004
Abbott, R. *et al.* (The LIGO Scientific Collaboration and the Virgo Collaboration) 2021c, *ApJL*, 913, L27
Abbott, R. *et al.* (The LIGO Scientific Collaboration and the Virgo Collaboration) 2021d, *ApJ*, 922, 71
Jaranowski P. and Krolak A. 2010, *Class. Quantum Grav.*, 27, 194015
Mastrogiovanni S. *et al.* 2017, *Class. Quantum Grav.*, 34, 135007
Middleton H. *et al.* 2020, *Phys. Rev. D*, 102, 023006
Suvorova S. *et al.* 2017 *Phys. Rev. D*, 96, 102006
Abbott, R. *et al.* (The LIGO Scientific Collaboration and the Virgo Collaboration) 2021e, *Phys. Rev. D* (in press); https://arxiv.org/abs/2109.09255
Abbott, R. *et al.* (The LIGO Scientific Collaboration, the Virgo Collaboration and the KAGRA Collaboration) 2021f, *Phys. Rev. Lett.* (submitted); https://arxiv.org/abs/2105.13085
Pierce A. *et al.* 2018, *Phys. Rev. Lett.*, 121, 061102
Piccinni O. *et al.* 2018, *Class. Quantum Grav.*, 36, 015008
Berge J. *et al.* 2018, *Phys. Rev. Lett.*, 120, 141101
Schlamminger S. *et al.* 2008, *Phys. Rev. Lett.*, 100, 041101
Reitze D. *et al.* 2019,
Punturo M. *et al.* 2010, *Class. Quantum Grav.*, 27, 194002

https://doi.org/10.1017/S1743921322002332 Published online by Cambridge University Press